

An Improved Method for Wind Measurements with a Conical-Scanning Correlation Lidar

Nobuo SUGIMOTO¹, Ichiro MATSUI¹, Mego PINANDITO², Takakazu ISHII³,
 Shigeru MURATA³ and Noboru YASUDA³

¹National Institute for Environmental Studies, 16-2 Onogawa, Tsukuba 305-0053, Japan

²Research and Development Center for Calibration, Instrumentation and Metrology, Indonesian Institute of Science (KIM-LIPI), Kompleks Puspitiek Serpong Tangerang, Indonesia

³NEC Corporation, 1-10 Nisshin-cho, Fuchu, Tokyo 189, Japan

(Received May 7, 1998; accepted for publication July 23, 1998)

An improved method using a conical-scanning correlation lidar was developed for wind measurements in the atmospheric boundary layer. The method is based on temporal correlation of lidar signals measured in multiple slant directions. In the new data analysis method, the number of calculation steps is approximately 1/8 of that of our previous method. The method was demonstrated using a compact Mie scattering lidar with a wedge prism conical scanner. The results were compared with simultaneous rawinsonde measurements. The measured wind profiles show qualitative agreement with the sonde data at altitudes where aerosol density is high.

KEYWORDS: wind, wind measurements, lidar, aerosol, time correlation, atmospheric boundary layer

1. Introduction

Various types of lidars have been developed for measuring wind velocity. These include coherent Doppler lidar, incoherent Doppler lidar, and scanning lidar based on the correlation method. The coherent heterodyne Doppler lidar method has been successfully used by many research groups including National Oceanic and Atmospheric Administration (NOAA) and National Aeronautics and Space Administration (NASA).¹⁾ Tropospheric wind measurements with the incoherent Doppler lidar method involve the use of high-spectral-resolution interferometers or filters.²⁾ The correlation lidar method has a simpler hardware system than that of the Doppler methods; however, it has some limitations such as the need for aerosol distributions with detectable structures for wind calculation.^{3–6)} In our previous paper, we reported a temporal correlation lidar which uses a conical scanner for measuring horizontal wind velocities in the atmospheric boundary layer.³⁾ Our aim was to develop a simple method for continuous measurements and which could be applied to a compact Mie scattering lidar and enhance its capabilities.

In this paper, we report an improved data analysis method for a conical-scanning temporal correlation lidar. The new method requires less calculation time and is better in judging the quality of the observed wind velocity data. We have tested the new algorithm using a vertical Mie scattering lidar with a wedge prism conical scanner, which was recently constructed for measuring urban atmospheric boundary layers.

2. Conical-Scanning Correlation Lidar Method

Wind measurements with a temporal correlation lidar are based on the experimental result that spatial autocorrelation of the horizontal distribution of aerosol has a single peak with a typical spatial scale of 100–1000 m. When temporal changes in aerosol density are measured at two locations, as illustrated in Fig. 1, the time lag between the temporal changes can be expressed by³⁾

$$T_m = (L/V) \cos(\phi - \phi_0), \quad (1)$$

where T_m represents time lag at the correlation peak, L is the distance between the measurement points, V is the wind speed, ϕ_0 is the wind direction, and ϕ is the direction from

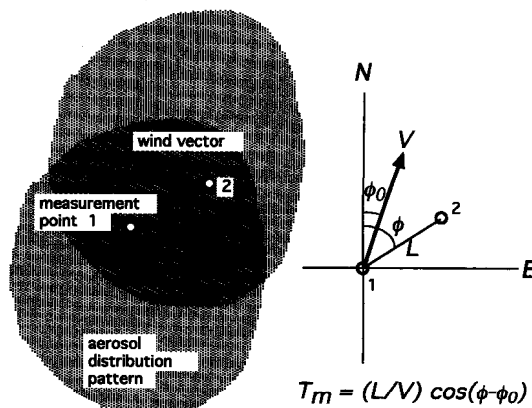


Fig. 1. Temporal correlation lidar method for measuring wind velocity.

one measurement point to another. It is assumed here that the aerosol distribution pattern moves with horizontal winds. It is also assumed that the vertical component of the wind is small, hence the aerosol pattern remains unchanged during the measurement period.

In the conical-scanning method, lidar signals are detected in multiple slant directions. There are five directions in the present system, as shown in Fig. 2. The temporal correlation of aerosol density is calculated as a function of the time lag for every combination of measurement points at each height.

Figure 3 is a diagram showing the directions along the pair of measurement points. There are five measurement points and ten combinations. The coordinate system (X , Y) in Fig. 3 indicates directions, and the unit of the scale is the same as for T_m/L or the inverse of wind speed (s/m). Equation (1) suggests that when we plot T_m/L along the measurement direction, the locations of the correlation peaks form a circle which passes through the origin, as shown in Fig. 3. We can then determine the wind speed and direction from the diameter and direction of the circle.³⁾ The direction of the circle is identified by the line that passes through the origin and center of the circle.

The correlation of the signals is defined by

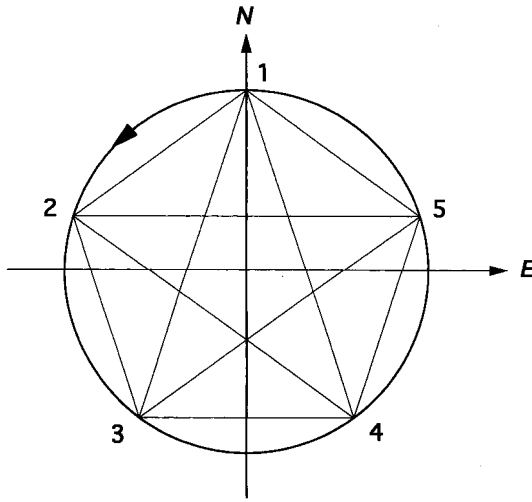


Fig. 2. Measurement directions and combinations of measurement points for calculating correlations.

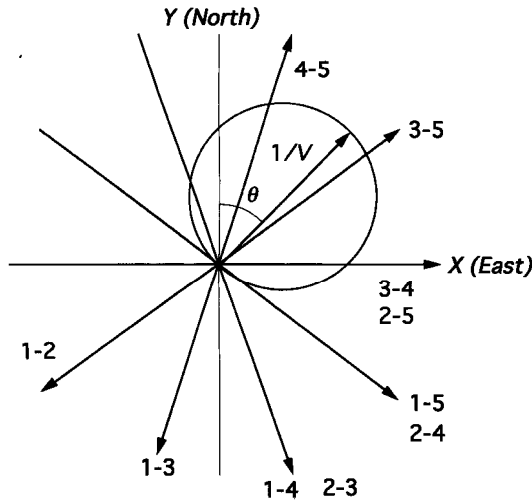


Fig. 3. Diagram for determining wind velocity.

$$R_{j-k,t} = \frac{1}{n-t} \sum_{i=1}^{n-t} \frac{(P_k(i) - \langle P_k \rangle)(P_j(i+t) - \langle P_j \rangle)}{\sigma_{P_j} \sigma_{P_k}}, \quad (2)$$

where $P_k(i)$ and $P_j(i)$ represent the temporal sequence of lidar signals measured at points k and j , and t is a positive time lag. σ_{P_j} and σ_{P_k} are defined by

$$\sigma_{P_j} = \sqrt{\langle (P_j(i) - \langle P_j \rangle)^2 \rangle}$$

$$\sigma_{P_k} = \sqrt{\langle (P_k(i) - \langle P_k \rangle)^2 \rangle}.$$

When the time lag is negative, the correlation is calculated in the same way by switching j and k .

In the algorithm presented in our previous work,³⁾ we calculated the correlation along each direction, plotted the time-lag peaks in the diagram shown in Fig. 3, and then fit a circle to the points. However, the calculation of correlations for all

time lags is very time-consuming and it is also difficult to weigh the contributions of the correlation peaks in the fitted circle and to evaluate the reliability of the determined wind velocity.

In the improved method presented in this paper, we first consider a circle that corresponds to a certain direction and a certain speed, then we calculate the sum of the correlation values at the points intersecting with the lines indicated in Fig. 3. We determine wind velocity by finding the best-fitted circle which has the largest value of the sum of the correlations. Here we must calculate the correlation only at the time lags required in the search process. Also, by taking the sum, the contributions of correlation measurements are weighted equally.

In the coordinate system in Fig. 3, a circle corresponding to the wind direction and speed (θ, V) has a center at (x_c, y_c) , where

$$x_c = (1/2V) \sin \theta,$$

$$y_c = (1/2V) \cos \theta. \quad (3)$$

The circle is expressed by

$$(x - x_c)^2 + (y - y_c)^2 = x_c^2 + y_c^2. \quad (4)$$

A line which passes through the origin and indicates the direction of the correlation measurement can be expressed by

$$ax + by = 0, \quad (5)$$

where the coefficient $b = 1$, and $a = \tan(2\pi/5)$, $\tan(2\pi/10)$, 0 , $\tan(-2\pi/10)$, and $\tan(-2\pi/5)$ for the lines in Fig. 3. The coordinates of the intersection between the line and the circle are calculated by

$$x = 2b(bx_c - ay_c)/(a^2 + b^2),$$

$$y = 2a(-bx_c + ay_c)/(a^2 + b^2). \quad (6)$$

The time lag corresponding to the point of intersection is expressed by

$$T/L = +r, \quad \text{if } x > 0$$

$$-r \quad \text{if } x < 0 \quad (7)$$

for the combinations of measurement points 1-4, 1-5, 2-3, 2-4, 2-5, 3-4, 3-5, and 4-5 where $r = \sqrt{(x^2 + y^2)}$, and

$$T/L = -r, \quad \text{if } x > 0$$

$$+r \quad \text{if } x < 0 \quad (8)$$

for 1-2 and 1-3. We should note that the commonly defined wind direction and the direction of the movement are opposite to each other. L , in eqs. (7) and (8), is the distance between the measurement points. L is calculated by

$$L = 2h \sin 36^\circ \tan \theta_s \quad (9)$$

for combinations 1-2, 1-5, 2-3, 3-4, and 4-5, where θ_s is the half-angle of conical scanning, and h is height.

$$L = 2h \cos 18^\circ \tan \theta_s \quad (10)$$

for combinations 1-3, 1-4, 2-4, 2-5, and 3-5.

To determine the best-fitted circle, we calculate the sum of the correlations for each trial circle. The sum is defined by

$$F(\theta, V) = \sum_{j,k} R_{j-k}(z)(\theta, V), \quad (11)$$

where j, k represent measurement points, of which there are 10 combinations. The correlations are calculated at the ten intersecting points. In the present work, we searched for the optimum (θ, V) considering 16 wind directions and 50 levels of wind speed.

3. Experiment and Discussion

The lidar system employs a compact Nd:YAG laser, the specifications of which are listed in Table I. The conical scanner uses a rotating wedge with a clear aperture of 25 cm. The angle of the conical scan is 5° in half-angle. It rotates twice per second, and the laser beam is transmitted in five directions with a repetition rate of 10 Hz. Photointerrupters are used to trigger the laser at the five rotational positions of the scanner, and an additional photointerrupter is used to identify direction 1. Lidar measurements were performed simultaneously with rawinsonde measurements. Rawinsondes were launched at 9:00, 12:00, 15:00, 18:00, and 21:00 JST on November 15, 1996 in Fuchu, Tokyo, and three lidar profiles were recorded for each time. In each lidar measurement, data were taken for 5 minutes with conical scanning to obtain a wind profile. Lidar signals were recorded for every single shot and stored on a hard disk. Using the method described in §2 the data analysis is done in an off-line mode.

Figure 4 shows aerosol profiles measured with the lidar at different times. Here the time-height indications (THI) of the aerosol measured for 5 min in direction 1 are presented. Diurnal variation of the boundary layer height is clearly seen in Fig. 4.

Figure 5 presents an example of temporal changes of the aerosol distribution measured in the five slant directions with conical scanning for 5 min. In this example taken at around 21:00 JST, aerosol concentration was found to be high in a height range from 1 km to 2.2 km. The temporal variations observed in different directions are similar, but there are slight time lags between them. Wind velocity is calculated from these time lags.

In Fig. 6 we show the range-corrected lidar signals (in direction 1) and their standard deviations for the measurements around 21:00 JST. Since the signal-to-noise ratio of the optical detection in the lidar system was sufficiently high, the standard deviations seen in Fig. 6 reflect changes in aerosol distribution, which can be used for the correlation analysis.

As described in the following sections, the correlation method performs very well when both signal intensity and standard deviation are high.

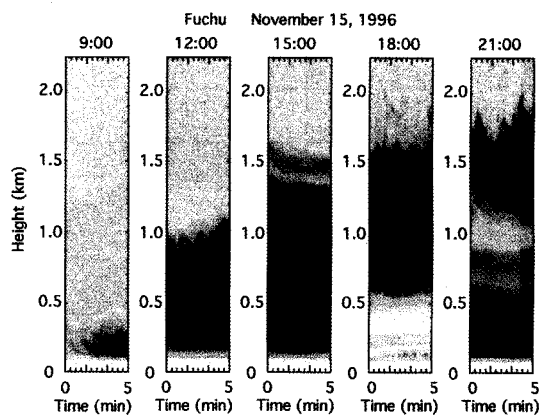


Fig. 4. Vertical profiles of aerosol at 9:00, 12:00, 15:00, 18:00, and 21:00 JST. Time-height indication during 5 min measured in direction 1 is shown. Dark areas indicate high aerosol density.

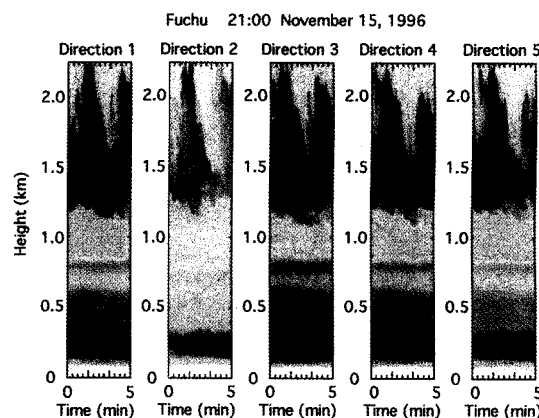


Fig. 5. Time-height indication in five slant directions at 21:00 JST.

Table I. Specifications of lidar system.

Laser	Compact Nd:YAG Laser
wavelength	$1.06 \mu\text{m}$
pulse energy	300 mJ
pulse repetition	10 Hz
Receiver telescope	
diameter	25 cm
Detector	Avalanche photodiode
Conical scanner	Wedge prism scanner
rotation	2/s
angle	5° (half-angle)
Transient digitizer	
signal bandwidth	10 MHz
sampling rate	20 MHz
accuracy	10 bits

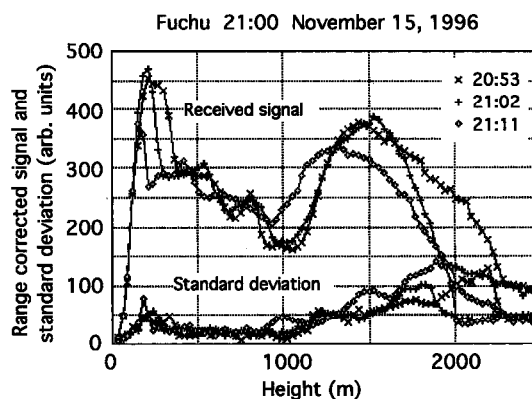


Fig. 6. Range-corrected lidar signals and standard deviations around 21:00 JST measured in direction 1.

Wind velocity was calculated every 30 m. We simply used zero-level corrected lidar signals to calculate correlations after averaging each 30 m range gate. We did not apply any inversion method or extinction correction to the signals in this work. A high-density structure such as a cloud having a high extinction coefficient may cause false correlation maxima at higher altitudes, but there was no evidence of this in the present data. In such a case, extinction correction is required.

Examples of the function $F(\theta, V)$ at several heights are shown in Fig. 7. $F(\theta, V)$ is normalized at the peak and indicated by a gray scale as a function of θ and V in the search area. The horizontal axis indicates 16 wind directions, and the vertical axis indicates 50 levels of wind speed. Dark areas indicate high $F(\theta, V)$. Well-defined peaks are obtained in these examples. The wind direction and speed are determined from the location of the peaks. At a height where there is no detectable structure in aerosol distribution, $F(\theta, V)$ does not show a clear peak. In such a case, we cannot determine the wind velocity. We can judge the quality of data from the contrast of the peak observed in Fig. 7 for $F(\theta, V)$. We have not considered the case where $F(\theta, V)$ does not show a clear single peak.

Wind velocity profiles obtained in our experiment are shown in Figs. 8(a) to 8(e). The measurement with sonde is indicated by a solid line in each figure. Wind velocity obtained with the lidar, only when $F(\theta, V)$ showed a well-defined peak, is plotted here. We obtained relatively good results in a height range where the aerosol density and the density variation were also high.

The result of the lidar measurement shows qualitative agreement with the sonde measurement, though sometimes there is a discrepancy as large as 90° in the wind direction. It is known that a sonde measurement may be erroneous because it is derived from only a single trajectory of the balloon flight. However, it seems that there is a systematic bias in the wind direction in Fig. 8. A bias can be caused if the spatial autocorrelation function of the aerosol distribution is not symmetrical with respect to the direction of the wind velocity, although it is not clear if this was the case. On comparing successive lidar profiles, deviation found to be mostly within ±45° for wind direction and ±2 m/s for wind speed. In the wind velocity estimate process shown in Fig. 7, errors were much smaller when well-defined peaks were obtained. The

standard deviation of θ and V for the five largest $F(\theta, V)$ in the search area was typically less than 10° and 1 m/s.

There are three parameters to be optimized in the measure-

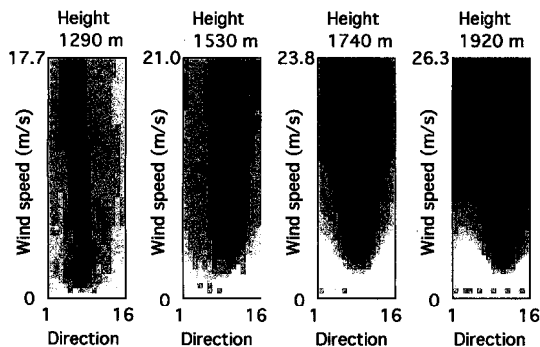
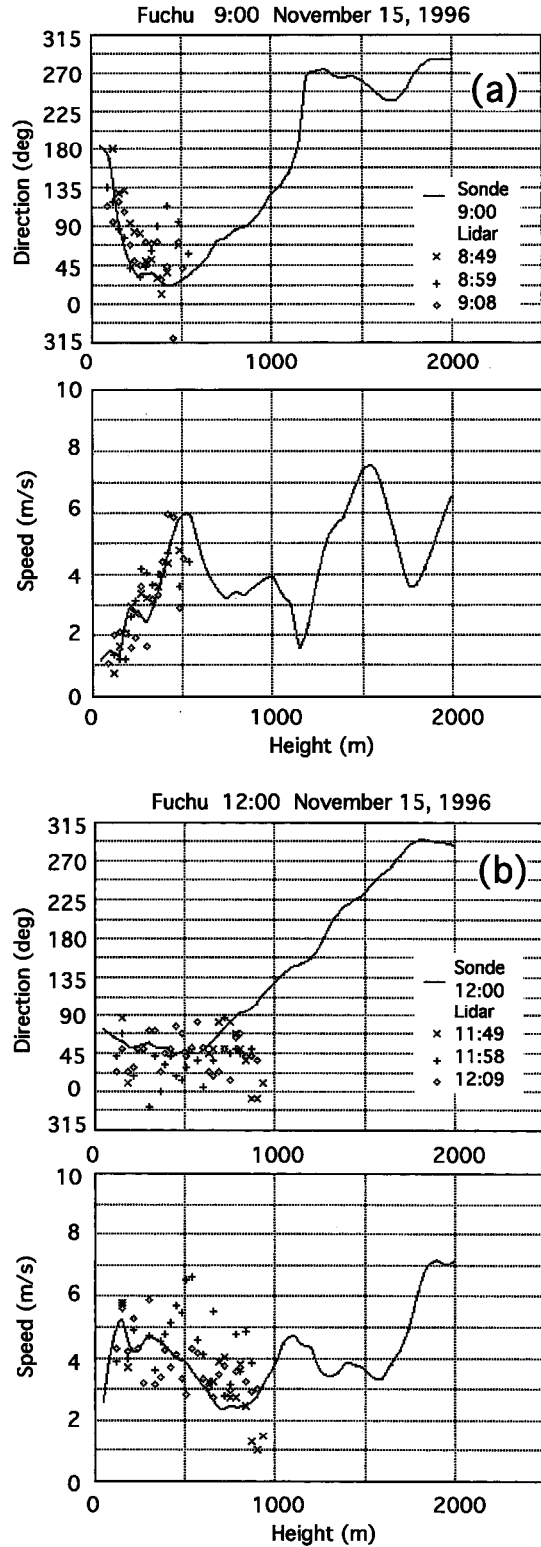


Fig. 7. $F(\theta, V)$ at several heights. $F(\theta, V)$ is normalized with the maximum and indicated by a gray scale in the search area as a function of θ and V .



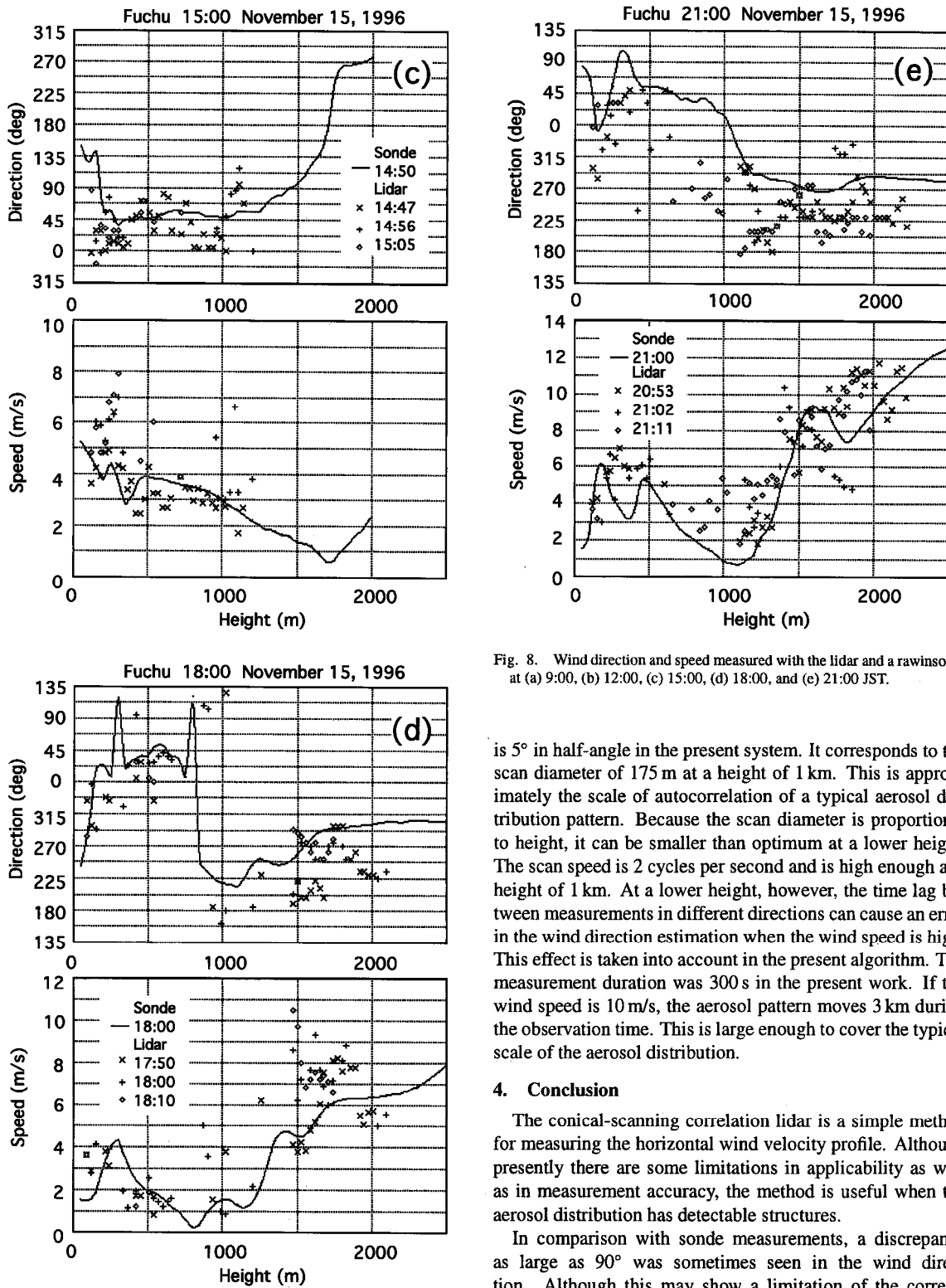


Fig. 8. Wind direction and speed measured with the lidar and a rawinsonde at (a) 9:00, (b) 12:00, (c) 15:00, (d) 18:00, and (e) 21:00 JST.

is 5° in half-angle in the present system. It corresponds to the scan diameter of 175 m at a height of 1 km. This is approximately the scale of autocorrelation of a typical aerosol distribution pattern. Because the scan diameter is proportional to height, it can be smaller than optimum at a lower height. The scan speed is 2 cycles per second and is high enough at a height of 1 km. At a lower height, however, the time lag between measurements in different directions can cause an error in the wind direction estimation when the wind speed is high. This effect is taken into account in the present algorithm. The measurement duration was 300 s in the present work. If the wind speed is 10 m/s, the aerosol pattern moves 3 km during the observation time. This is large enough to cover the typical scale of the aerosol distribution.

4. Conclusion

The conical-scanning correlation lidar is a simple method for measuring the horizontal wind velocity profile. Although presently there are some limitations in applicability as well as in measurement accuracy, the method is useful when the aerosol distribution has detectable structures.

In comparison with sonde measurements, a discrepancy as large as 90° was sometimes seen in the wind direction. Although this may show a limitation of the correlation method, the method is still useful as a continuous measurement method which is complementary to sonde measurements. Such continuous measurements can provide useful data in the study of the structure and movement of the atmospheric boundary layer.

ment method. They are the angle of the conical scan, the scan speed, and the duration of the measurement. These parameters were set based on our previous results.³⁾ The scan angle

The data analysis method presented in this paper requires less calculation time than our previous method because correlation is calculated only at the limited time lags which are required in wind velocity estimations. The number of calculation steps was approximately 1/8 of that of our previous method. It took approximately 6 min, using a personal computer with a 200 MHz CPU, to calculate correlations, display the graphs of $F(\theta, V)$, and estimate wind velocity at 60 altitudes.

The Mie scattering lidar system used in the present study is operated in Jakarta, Indonesia, for the study of air pollution in Jakarta. We plan further investigations on the air pollution in Jakarta using the correlation lidar method.

Acknowledgements

A part of this work was carried out as a part of the cooperative program of the New Energy and Industrial Technology Development Organization (NEDO) of Japan and the Indonesian Institute of Science (LIPI) of the Republic of Indonesia.

- 1) J. G. Hawley, R. Targ, S. W. Henderson, C. P. Hale, M. J. Kavaya and D. Moerder: *Appl. Opt.* **32** (1993) 4557.
- 2) K. W. Fischer, V. J. Abreu, W. R. Skinner, J. E. Barnes, M. J. McGill and T. D. Irgang: *Opt. Eng.* **34** (1995) 499.
- 3) I. Matsui, N. Sugimoto, Y. Sasano and H. Shimizu: *Jpn. J. Appl. Phys.* **29** (1990) 441.
- 4) J. L. Schols and E. W. Eloranta: *J. Geophys. Res.* **97** (1992) 18395.
- 5) S. Sutton and M. Bennett: *Int. J. Rem. Sens.* **15** (1994) 375.
- 6) V. E. Zuev, V. S. Komarov and A. V. Kreminskii: *Appl. Opt.* **36** (1997) 1906.